

Phase Transitions

Synthesis, Thermal Behavior, and Dehydrogenation Kinetics Study of Lithiated Ethylenediamine

Juner Chen,^[a, b] Guotao Wu,^[a] Zhitao Xiong,^[a] Hui Wu,^[c, d] Yong Shen Chua,^[a] Wei Zhou,^[c, d] Bin Liu,^[a] Xiaohua Ju,^[a] and Ping Chen^{*[a]}

Abstract: The lithiation of ethylenediamine by LiH is a stepwise process to form the partially lithiated intermediates $\text{LiN(H)CH}_2\text{CH}_2\text{NH}_2$ and $[\text{LiN(H)CH}_2\text{CH}_2\text{NH}_2]_n$ prior to the formation of dilithiated ethylenediamine $\text{LiN(H)CH}_2\text{CH}_2\text{N(H)Li}$. A reversible phase transformation between the partial and dilithiated species was observed. One dimensional $\{\text{Li}_n\text{N}_n\}$ ladders and three-dimensional network structures were found in the crystal

structures of $\text{LiN(H)CH}_2\text{CH}_2\text{NH}_2$ and $\text{LiN(H)CH}_2\text{CH}_2\text{N(H)Li}$, respectively. $\text{LiN(H)CH}_2\text{CH}_2\text{N(H)Li}$ undergoes dehydrogenation with an activation energy of $181 \pm 8 \text{ kJ mol}^{-1}$, whereas the partially lithiated ethylenediamine compounds were polymerized and released ammonia at elevated temperatures. The dynamical dehydrogenation mechanism of the dilithiated ethylenediamine compounds was investigated by using the Johnson-Mehl-Avrami equation.

Introduction

Metalated amines, a class of organometallic compound, are useful raw chemicals and catalysts in organic and organometallic chemistry.^[1] In particular, lithiated amines play an indispensable role in the widespread use of all other metalated amines because these compounds are important reagents frequently used to transfer the amido ligand in the synthesis of other metalated amines throughout the Periodic Table. Lithiated amines are more stable and soluble than the other metalated amines and are powerful Brønsted bases, which are the preferred bases for the formation of ketone enolates.^[2] Ever increasing research activities concerning the actions and structures of lithiated amines have emerged.^[3] The ease of use and high reactivity have led lithiated amines to be one of the most regularly used reagents in synthetic chemistry. In practice, reagents derived from lithiated secondary amines $[(\text{R}_2\text{NLi})_n]$ are

widely used. As examples, lithiated diisopropylamine (LDA), lithiated 2,2,6,6-tetramethylpiperidine (LTMP), and lithiated hexamethyldisilazane (LiHMDS) are the bases of choice for a number of enolization, ortholithiation, and epoxide lithiation reactions.^[4] In contrast, lithiated primary amines $[\{\text{RN(H)Li}\}_n]$ have received relatively little attention as bases, although a variety of these compounds have been structurally characterized.^[5] Admittedly, many organolithium reactions demand fully aprotic conditions, and a number of investigators (most notably Seebach) have shown that protic amine byproducts derived from hindered lithiated amines can be detrimental in the reactions of enolates.^[6] Nevertheless, there are many stabilized carbanions and related organolithium intermediates that can tolerate weak protic conditions. Primary amines and the corresponding protic lithiated amines have been investigated in the fields of organolithium-mediated polymerization,^[7] epoxide cleavage,^[8] metalation,^[9] and have potential in asymmetric syntheses.^[10]

Polymeric/cyclic oligomeric aggregates that feature $\{\text{Li}_n\text{N}_n\}$ ladder cores have been the preferential aggregation mode for lithiated amine species by using extensive ab initio molecular-orbital calculations on the unsolvated and solvated model compounds.^[11] Difficulties in understanding the association of such species are due to the limited crystallographic information concerning polymeric amides; most lithiated amines form monomers or oligomers, including dimers, trimers, tetramers, and hexamers.^[12] The structures of lithiated oligomeric and polymeric ethylenediamine (EDA) compounds were recently determined to favor ladder structures over stacked dimers based on extensive ab initio molecular-orbital calculations.^[13]

There have been a number of studies on the thermal decomposition of alkyllithium compounds. The mechanism of such a decomposition is widely believed to be α,β -hydride elimination, thus yielding lithium hydride and the appropriate

[a] J. Chen, Dr. G. Wu, Prof. Z. Xiong, Dr. Y. S. Chua, B. Liu, X. Ju, Prof. P. Chen
Dalian National Laboratory for Clean Energy
Dalian Institute of Chemical Physics
Chinese Academy of Sciences, Dalian 116023 (P.R. China)
Fax: (+86)411-84379583
E-mail: pchen@dicp.ac.cn

[b] J. Chen
University of Chinese Academy of Science
Beijing, 100049 (P.R. China)

[c] Dr. H. Wu, Dr. W. Zhou
NIST Center for Neutron Research
National Institute of Standards and Technology
Gaithersburg, Maryland, 20899-6102 (USA)

[d] Dr. H. Wu, Dr. W. Zhou
Department of Materials Science and Engineering
University of Maryland, College Park, Maryland, 20742-2115 (USA)

Supporting information for this article is available on the WWW under <http://dx.doi.org/10.1002/chem.201403047>.

alkene.^[14] Similarly, lithiated secondary amines, such as lithiated dimethylamine, lithiated diethylamine, and lithiated diisopropylamine decompose, probably through an α,β -lithium hydride elimination mechanism to give *N*-methylenemethylamine, *N*-ethylideneethylamine, and *N*-isopropylideneisopropylamine, respectively.^[15] Interestingly, our recent experimental results show that lithiated primary amines release H₂ rather than LiH at moderate temperatures, which is likely due to the presence of an α -hydrogen atom at the nitrogen site.^[16] This new finding shows that lithiated primary amines have the potential to be hydrogen carriers.

Herein, we focus on the investigation of lithiated ethylenediamine, including the synthetic method, thermal behavior, and dehydrogenation kinetics. A phase transfer between the partial and dilithiated species during the synthesis was observed, which clearly evidences a stepwise lithiation of EDA. The thermal decomposition properties of partial and dilithiated EDA were studied. The kinetic investigation shows that there are two different rate-determining processes in the different dehydrogenation stages of dilithiated EDA.

Experimental section

Synthesis

LiH (98%, Alfa Aesar)^[22] and EDA (EDA, 99.5%; Fluka) are commercial products and were used without further purification. Monolithiated EDA (LiEDA) was prepared by ball milling LiH and EDA in a molar ratio of 1:1 in a Retsch PM 400 planetary mill at 200 rpm and room temperature for 2 h. The partially lithiated EDA intermediate [LiEDA][Li₂EDA]₂ was prepared by heating LiEDA in an open vessel in an argon flow at 100 °C for 4 h. Dilithiated EDA (Li₂EDA) was prepared by ball milling LiH and EDA in a molar ratio of 2:1 at 200 rpm at 60 °C for 24 h followed by a heat treatment at 130 °C for 4 h. Mixtures of LiEDA/LiH and LiEDA/3LiH were prepared by ball milling LiH and EDA in molar ratios of 2:1 and 4:1 at 200 rpm at room temperature for 2 h, respectively. Sample mixtures (ca. 600 mg) were loaded into a 180 mL vessel and milled. The ball-to-powder ratio was 50:1. Heat treatments of the premilled samples of LiEDA/LiH and LiEDA/3LiH were conducted by using a Sievert-type apparatus. Samples (100 mg) were heated inside a closed chamber. All the sample handling was performed in an MBRAUN 200 glovebox filled with purified argon (O₂ and H₂O concentrations were below 1 ppm).

Characterization

X-ray diffraction studies were conducted on a PANalytical X'pert diffractometer (Cu_{K α} radiation, 40 kV, 40 mA). A cell was used in situ to avoid sample exposure to air during the measurement. High-resolution X-ray diffraction patterns were collected at room temperature at the BL14B1 beamline of Shanghai Synchrotron Radiation Facility (SSRF; Shanghai, China). Thermogravimetric and differential thermal analysis (TG-DTA) measurements were carried out on a Netzsch TG-DTA apparatus (Netzsch, Germany). A sample (10 mg) was heated in Al₂O₃

crucibles at 1 °C min⁻¹ in an argon flow. Hydrogen-desorption measurements were performed by means of a homemade temperature-programmed desorption (TPD) system that comprised a microreactor and a mass spectrometer (Hiden HPR-20). Quantitative measurements of hydrogen desorption from lithiated EDA were conducted on a Sievert-type apparatus. Samples (100 mg) were heated inside a closed chamber (heating rate = 2 °C min⁻¹). The pressure increase in the chamber was monitored and small amounts of gaseous product were conducted from the pressurized chamber to the mass spectrometer for analysis at heating intervals. FTIR spectra were recorded on a Varian 3100 unit.

Results and discussion

Synthesis of lithiated EDA

Compounds rich in protic hydrogens, such as NH₃, N₂H₄, and LiNH₂, are expected to react with hydridic hydrogen atoms in metal hydrides to generate H₂ due to the interaction between the oppositely charged H ^{δ +} and H ^{δ -} atoms.^[17] Ethylenediamine (NH₂CH₂CH₂NH₂), the simplest diamine, possesses four partially positively charged hydrogen atoms and has the potential to react with metal hydrides. Thus, we mixed EDA and LiH in different molar ratios (EDA/LiH = 1:1, 1:2, and 1:4) to understand the reactivity between these compounds. As expected, the release of H₂, which was identified by mass-spectrometric analysis (see Figure S1 in the Supporting Information), took place easily by ball milling the EDA/LiH mixture in a molar ratio of 1:1 at room temperature. Monitored by a pressure gauge, one equivalent of H₂ was released during the ball-milling process. It is likely that EDA reacts with equivalent of LiH and gives rise to monolithiated EDA (LiEDA; LiNHCH₂CH₂NH₂) and H₂ following reaction (1).



The solid residue has a diffraction pattern that matches the previously reported LiEDA well (Figure 1 b, left).^[18] Kowach and co-workers found that LiEDA can be synthesized by an acid-base reaction of Li₃N, LiNH₂, or *n*BuLi with excess EDA at room temperature. Based on the XRD data, the crystal structure of LiEDA can be well matched to a monoclinic structure (space group *P*₂₁/*n*) with lattice parameters of approximately *a* = 12.943(1), *b* = 9.259 (4), *c* = 13.870 (4) Å, and β = 103.303° (Table 1). The structure of LiEDA consists of infinite one-dimensional ladders of double-edge-sharing LiN₄ tetrahedra (such that a common vertex is shared) formed from -NH₂ and -NH bonding interactions (Figure 2a). The ladders run parallel to the crystallographic *c* axis and are effectively isolated from one another because the EDA molecules in a given chain are bent into the chain (Figure 2b). The bonding between the lithium atom and the -NH group of the EDA constructs the frame of a ladder with a sinusoidal ribbonlike pattern, as viewed from the side of the ladder. Two bonding environments of the ligand are present. The {Li₂N₂} rings are rotated so that the -NH and -NH₂ groups of the same EDA ligand are bonded to

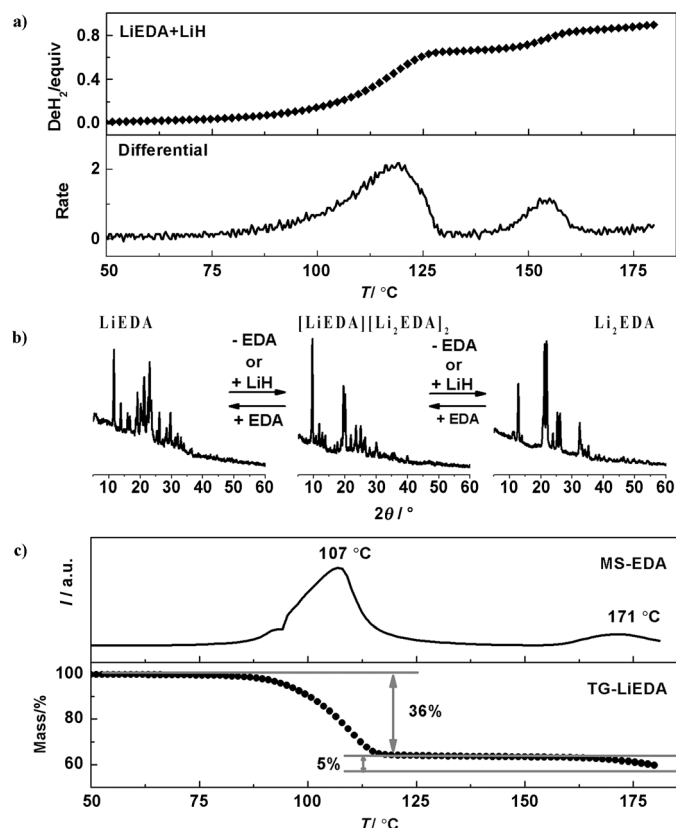


Figure 1. a) Volumetric gas-release curve and the differentiated line for the LiEDA/LiH mixture heated from RT to 180 °C in a closed vessel; b) XRD patterns of LiEDA, [LiEDA][Li₂EDA]₂, and Li₂EDA, respectively; c) TG curve and the corresponding TPD-MS spectrum (EDA signal) of LiEDA heated from RT to 180 °C in an argon flow. The ramping rate for the volumetric release and TG analysis was 2 °C min⁻¹.

Table 1. Summary of crystal parameters of LiEDA and Li ₂ EDA.		
Parameters	LiEDA	Li ₂ EDA
Formula	C ₂ H ₇ LiN ₂	C ₂ H ₆ Li ₂ N ₂
M _r [g mol ⁻¹]	66.03	71.96
Crystal system	monoclinic	monoclinic
Space group	P2 ₁ /n (No.14)	C12/c1 (No.15)
a [Å]	12.943(1)	11.1282(15)
b [Å]	9.259 (4)	12.5185(18)
c [Å]	13.870 (4)	8.0692(11)
β [°]	103.303(0)	134.0218(32)

the lithium atoms in the form of either rings or a frame of the ladder in an alternating fashion. The bonding in LiEDA is primarily ionic in character with Li–N bonds formed through interactions with the –NH group and covalent bonds through the lone pair of electrons on the –NH₂ group. In the structure of LiEDA, the monoprotonated nitrogen atom is penta-coordinated (3×Li, 1×H, and 1×C). This hyper-coordination, although unusual, has been observed in several amides, for example, a penta-coordinated nitrogen atom with 3×Li and 2×H in LiNH₂.^[19] In contrast, the diprotonated nitrogen atom of the EDA ligand forms a dative bond with the lithium atom lying in a tetrahedral coordination.

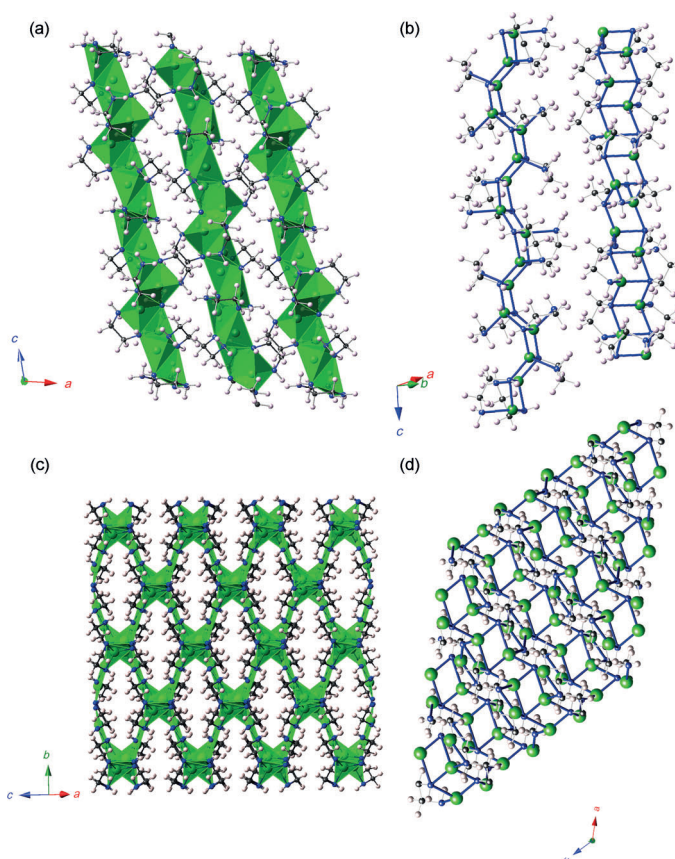
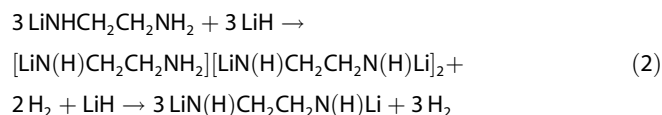


Figure 2. a) Crystal structure of LiEDA; b) [Li_nN_n] ladders in LiEDA; c) crystal structure of Li₂EDA; and d) [Li_nN_n] ladders in Li₂EDA. The Li, N, C, and H atoms are represented as green, blue, black, and pink spheres, respectively.

The addition of one more mole of LiH into the EDA/LiH mixture leads to further dehydrogenation and the formation of dilithiated EDA (i.e., Li₂EDA (Li(H)CH₂CH₂N(H)Li)). However, the dehydrogenation kinetics are poor, as reported previously by us.^[16] An optimal ball-mill and heat-treatment method was applied in this study to save the reaction time and synthesize well-crystalline Li₂EDA. Ball milling the EDA/2LiH mixture for a short period of time (2 hours) gave rise to the mixture of LiEDA and LiH, which was further heated from room temperature to 180 °C in a closed vessel (see Figure S2 in the Supporting Information). A two-step dehydrogenation process occurred (see Figure 1 a and Figure S3 in the Supporting Information). About 0.67 equivalents of H₂ were released from the LiEDA/LiH mixture in the first step, thus leading to the formation of a structure-unknown intermediate with the chemical composition of [LiEDA][Li₂EDA]₂ (Figure 1 b, middle). When heating to 175 °C, 0.9 equivalents of H₂ evolve with the formation of Li₂EDA. However, Li₂EDA decomposes easily at such a high temperature. To obtain high-purity Li₂EDA, we held the premilled EDA/2LiH sample (ball milled at 60 °C for 24 h with the release of 1.3 equivalents of H₂) at 130 °C for 4 hours (see Figure S4 in the Supporting Information). Well-crystalline Li₂EDA can be collected after releasing the remaining 0.6 equivalents of H₂ (Figure 1 b, right). The overall lithiation process is described in Equation (2). A similar phase transfor-

mation from monolithiated amine to dilithiated amine with the formation of an intermediate was observed in the synthesis of the lithiated *N,N*-di-*tert*-butylethylenediamine.^[13] The crystal structures of the partial lithiated amines provided mechanistic information on the formation of the $\{Li_nN_n\}$ ladder and direct evidence for the assembly of polymeric structures in amidolithium chemistry. The dilithiated species can be isolated into two forms that exhibit either a dimeric $\{Li_4N_4\}$ cage or possibly a polymeric $\{Li_nN_n\}$ ladder. However, the association with a linear polymeric species showed excellent internal agreement and clearly placed aggregation to a polymeric ladder, which is more favorable relative to a stacked dimeric species.

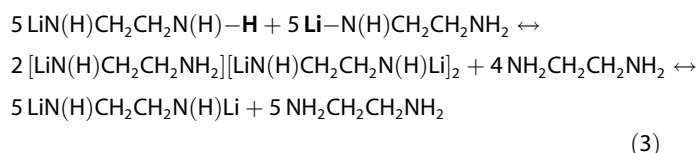


The crystal structure of Li_2EDA was determined by using high-resolution XRD data and is well matched to a monoclinic structure with lattice parameters of approximately $a = 11.128(1)$, $b = 12.518(1)$, $c = 8.069(1)$ Å, $\beta = 134.022(3)^\circ$, and $V = 808.3(1)$ Å³ (Table 1). Although the structure was reported before by using ab initio molecular orbital calculations,^[13] a detailed analysis was not given. Similar to the structure of LiEDA, $\{Li_2N_2\}$ rings are also observed in Li_2EDA . The spatial connection of such $\{Li_2N_2\}$ rings leads to the formation of an infinite three-dimensional network (Figure 2c). The $\{Li_nN_n\}$ ladders expand in all directions and are cross-linked with each other (Figure 2d), thus forming a cagelike structure (viewed along the c axis as shown in Figure S5; see the Supporting Information). Half of the lithium atoms in a $\{Li_2N_2\}$ ring (Li1) are tetrahedrally bonded with two pairs of $-\text{NH}$ groups in two different EDA ligands, thus forming two Li-N-C-C-N pentagon rings. The Li-N edges of these pentagons serve as building blocks to constitute the three-dimensional $\{Li_nN_n\}$ ladders. In contrast, Li2 only acts as a joint to connect three neighboring individual Li-N-C-C-N pentagons and form the frame of the $\{Li_nN_n\}$ ladder. Therefore, there are two different coordination environments of lithium ions in Li_2EDA , that is, the $\{LiN_4\}$ tetrahedra and $\{LiN_3\}$ triangle (see Figure S6a in the Supporting Information). The bonding in Li_2EDA is primarily ionic in character with Li-N bonds formed through the interaction with the $-\text{NH}$ group. All the EDA ligands participate in the formation of the Li-N-C-C-N pentagon rings through bonding with the lithium ions. Hyper-coordination of the nitrogen atoms was also found in Li_2EDA . One terminal nitrogen atom (N4) in an EDA ligand is penta-coordinated with $3 \times \text{Li}$, $1 \times \text{H}$, and $1 \times \text{C}$ atoms, similar to the coordination environment of the monoprotonated nitrogen atom in LiEDA (see Figure S6b in the Supporting Information). Although the other terminal nitrogen atom (N3 in Figure S6b) in the same EDA ligand even shows hexa-coordination with $4 \times \text{Li}$, $1 \times \text{H}$, and $1 \times \text{C}$ atoms. The most important distances in the structure of Li_2EDA are summarized in Table S1 (see the Supporting Information).

However, there are still two more protic hydrogen atoms in the dilithiated EDA. To confirm whether Li_2EDA reacts further

with LiH, we ball milled EDA with 4 equivalents of LiH followed by heat treatment. The EDA/4LiH mixture only gave rise to a mixture of Li_2EDA and LiH (see Figure S7 in the Supporting Information).

Interestingly, a reversible phase transformation between the partially lithiated and dilithiated EDA occurred when heating LiEDA in an argon flow. As shown in the TG curve (Figure 1c), detachments of 0.4 and 0.06 equivalents of EDA (evidenced by mass-spectrometric analysis) from LiEDA in two stages led to the formation of $[\text{LiEDA}][\text{Li}_2\text{EDA}]_2$ and Li_2EDA , respectively. Therefore, pure $[\text{LiEDA}][\text{Li}_2\text{EDA}]_2$ can be synthesized by heating LiEDA in an argon flow at 100°C for 4 hours. On the other hand, LiEDA reformed by dissolving Li_2EDA into excess EDA. Thus, it is proposed that a reversible transformation of partial and dilithiated EDA can be achieved through an exchange between Li^+ ions and the active protic hydrogen atom in the $-\text{NH}_2$ group [Eq. (3)].



Thermal decomposition of lithiated EDA

Our previous work on the thermal decomposition of Li_2EDA demonstrated that two equivalents of H_2 can be released upon holding the sample at 180°C .^[16] It is interesting to investigate the thermal decomposition of the partially lithiated EDA compounds. We performed volumetric-release measurements in a closed system to understand the thermal behavior of LiEDA and $[\text{LiEDA}][\text{Li}_2\text{EDA}]_2$ relative to Li_2EDA .

About 1.2 and 1.8 equivalents of gaseous products per EDA molecule were released from LiEDA and $[\text{LiEDA}][\text{Li}_2\text{EDA}]_2$, respectively (Figure 3a). Different from Li_2EDA , a two-step decomposition of LiEDA or $[\text{LiEDA}][\text{Li}_2\text{EDA}]_2$ was observed, as shown in the differential results (Figure 3b). Mass-spectrometric analysis showed that H_2 and NH_3 are the main gaseous products for LiEDA and H_2 , NH_3 , and C_xH_y species for $[\text{LiEDA}][\text{Li}_2\text{EDA}]_2$. Li_2NH and an unknown phase were observed in the decomposition residue of LiEDA. However, only a weak peak for Li_2CN_2 was found in the product of $[\text{LiEDA}][\text{Li}_2\text{EDA}]_2$.

LiEDA, as mentioned above, detaches EDA through the exchange of Li^+ and $\text{H}^{\delta+}$ ions in the $-\text{NH}_2$ group in an argon flow or under vacuum [Eq. (3)]. When loading the sample into a closed system, dehydrogenation followed by the release of ammonia took place at elevated temperatures (evidenced by mass-spectrometric analysis; see Figure S8 in the Supporting Information). However, the decomposition of $[\text{LiEDA}][\text{Li}_2\text{EDA}]_2$ seems more complicated with the desorption of H_2 , NH_3 , and C_xH_y species. The above results indicate that LiEDA and $[\text{LiEDA}][\text{Li}_2\text{EDA}]_2$ may go through different decomposition pathways from that of Li_2EDA . However, the decomposition mechanisms of partial lithiated EDA compounds are still unclear and need further study. As dilithiated EDA releases high-

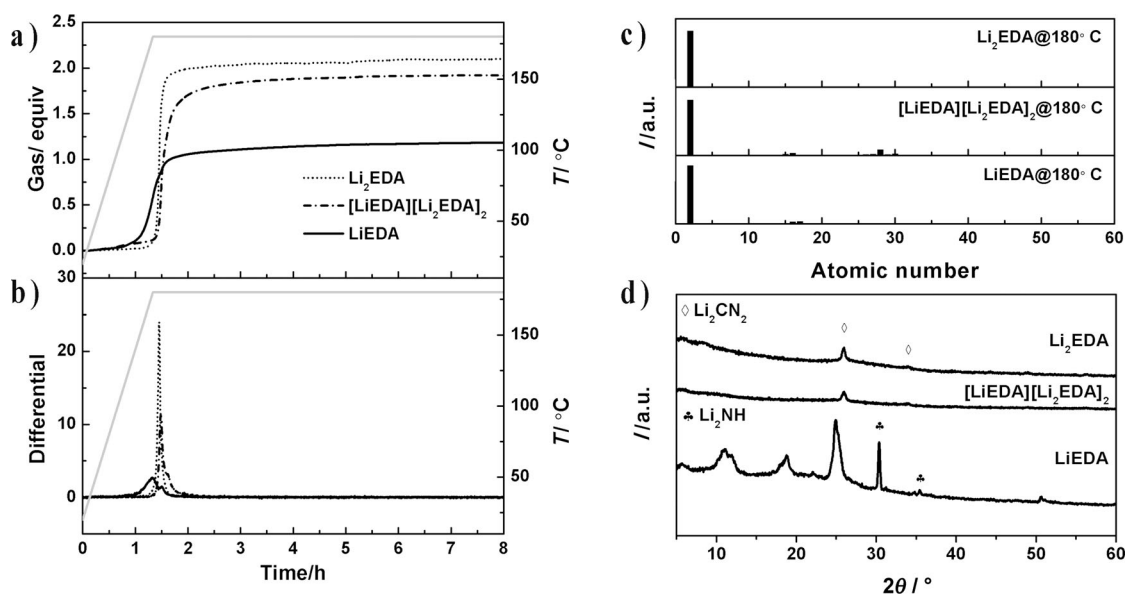


Figure 3. a) Volumetric release curves of Li₂EDA, [LiEDA][Li₂EDA]₂, and Li₂EDA; b) differential results of the decomposition processes; c) MS analyses of the gaseous products; d) XRD patterns of the decomposition residues.

purity hydrogen gas at around 180 °C, the dehydrogenation kinetics are investigated further in the following section.

Kinetic studies of hydrogen release from Li₂EDA

The Kissinger method [Eq. (4)] was employed to determine the energy barrier in hydrogen desorption from Li₂EDA.

$$\ln(\beta/T_p^2) = -E_a/RT_p + \ln(AR/E_a) \quad (4)$$

in which T_p is the temperature at which the maximum reaction rate peaks, β is the heating rate, E_a is the activation energy, A is the pre-exponential factor, and R is the gas constant. The maximum reaction-rate temperatures at different heating rates were collected by means of differential scanning calorimetry (DSC) measurements. The DSC profiles of hydrogen desorption from Li₂EDA at different ramping rates are shown in Figure 4a. It was observed that the peak temperatures shifted monotonically to higher values when the ramping rate was increased from 0.1 to 0.5 °C min⁻¹. The dependence of $\ln(\beta/T_p^2)$ to $1/T_p$ was plotted (Figure 4b). The slope and intercept of the fitted line were used to determine the values of E_a and A , respectively. Once E_a and A are known, the specific rate constant k at given temperature can be calculated by the Arrhenius equation:

$$k = A \exp(-E_a/RT) \quad (5)$$

The values of E_a , A , and k (at 130, 150, 165, and 180 °C) for Li₂EDA are shown in Table 2. As mentioned above, the rate constant k rises rapidly with increasing reaction temperature. The activation energy E_a for the hydrogen desorption from Li₂EDA is around 181 ± 8 kJ mol⁻¹.

Such a high activation energy means that 1) the dehydrogenation reaction is temperature sensitive; in other words,

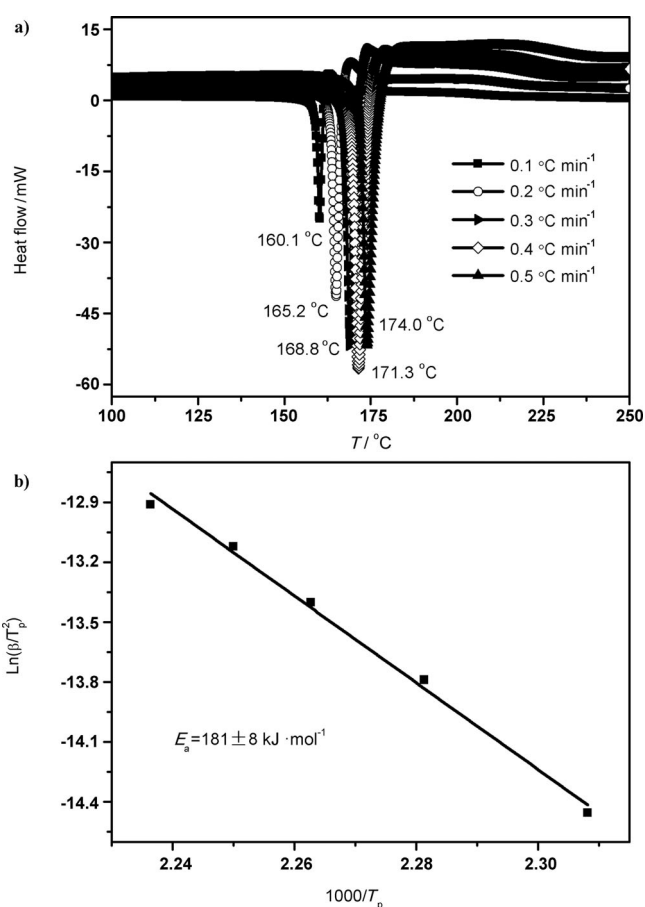


Figure 4. a) DSC profiles of hydrogen desorption from Li₂EDA at ramping rates of 0.1, 0.2, 0.3, 0.4, and 0.5 °C min⁻¹; b) Kissinger plots, which give the activation energy of Li₂EDA.

Sample	E_a [kJ mol ⁻¹]	A [min ⁻¹]	T [°C]	k [min ⁻¹]
Li ₂ EDA	181 ± 8	7.5 × 10 ¹⁹	130	2.6 × 10 ⁻⁴
			150	2.3 × 10 ⁻³
			165	2.0 × 10 ⁻²
			180	1.0 × 10 ⁻¹

temperature is one of the most important factors to affect the dehydrogenation rate; 2) the energy barrier to the formation of the transition state is high. To understand the significance of temperature and find out the dynamic mechanism of dehydrogenation, we performed combined isothermal dehydrogenation experiments at different temperatures and used the Johnson-Mehl-Avrami (JMA) method.

Isothermal dehydrogenation reactions of Li₂EDA were carried out at four different temperatures for comparison (Figure 5 a). It takes 152.8, 20.2, 1.11, and 0.15 hours to liberate two equivalents of H₂ from Li₂EDA upon heating at 130, 140, 165, and 180 °C, respectively (Table 3). The corresponding highest dehy-

drogenation rates calculated from the first-order differential results are 0.16, 1.4, 7.9, and 48.7 mol h⁻¹, respectively (Figure 5b). A linear relationship between ln(V_{max}) and the derivative of the operation temperature (1/ T) was found (Figure 5c). Obviously, the active energy of the Li₂EDA dehydrogenation can also be obtained from the slope (i.e., $E_a = 173 \pm 7$ kJ mol⁻¹, which is close to the value obtained from the Kissinger method ($E_a = 181 \pm 8$ kJ mol⁻¹).

It is well known that the kinetic model for the isothermal dehydrogenation of solid materials can be expressed by using Equation (6):

T [°C]	t [h]	V_{max} [mol h ⁻¹]	Avrami exponent [n]	
130	152.8	0.16	0 < α ≤ 0.25	0.25 < α < 1
150	20.2	1.4	1.0	5.9
165	1.11	7.9	0.5	3.5
180	0.15	48.7	0.6	4.0

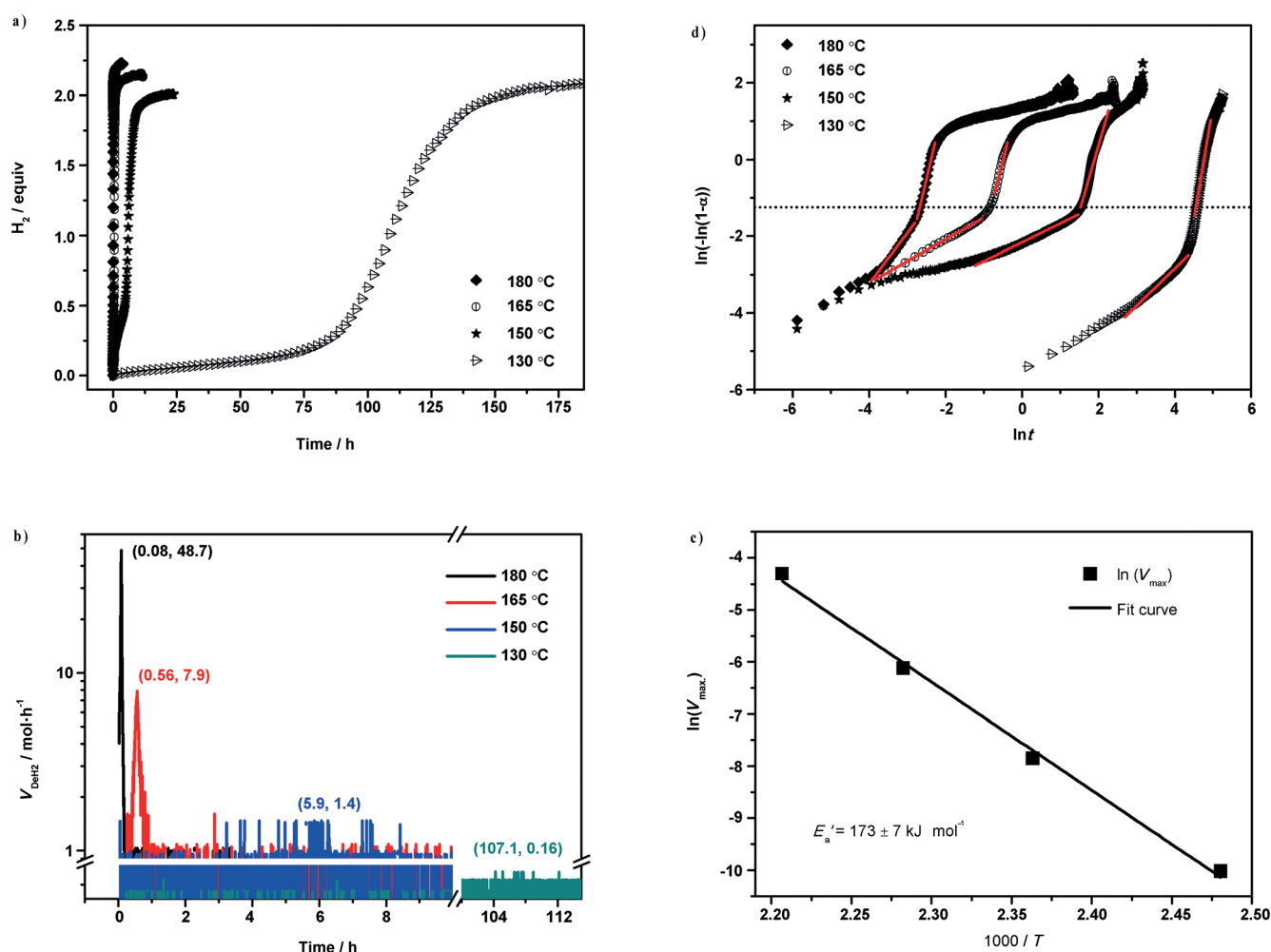


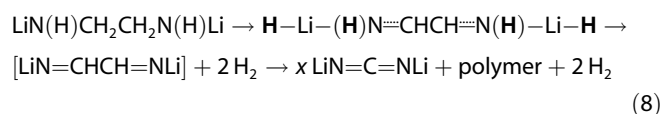
Figure 5. a) Isothermal dehydrogenation of Li₂EDA at 130, 150, 165, and 180 °C, respectively; b) first-order differential results of (a); c) relationship of ln(V_{max}) versus 1/ T ; d) results from the JMA method for Li₂EDA.

$$\alpha(t) = 1 - \exp[-(kt)^n] \quad (6)$$

in which $\alpha(t)$ is the fraction that has already reacted at time t (range = 0–1), t is the reaction time, k is the rate constant, and n is the Avrami exponent. The JMA equation was widely used to describe the time-dependent kinetic behavior for isothermal solid-state reactions,^[20] in which the Avrami exponent n represents the nucleation and growth process. In practical applications, Equation (6) is generally rearranged as

$$\ln\{-\ln[1-\alpha(t)]\} = n\ln(t) + n\ln(k) \quad (7)$$

By plotting $\ln\{-\ln[1-\alpha(t)]\}$ versus $\ln(t)$, the Avrami exponent n and rate constant k can be obtained from the slope and intercept of the straight line. We plotted $\ln\{-\ln[1-\alpha(t)]\}$ against $\ln(t)$ in the range $0 < \alpha < 1$ for Li_2EDA (Figure 5d).^[21] It can be seen that the value of n for Li_2EDA was lower than 1.3 in the range $0 < \alpha \leq 0.25$, which corresponds to a diffusion-controlled reaction mechanism in the initial stage.^[21] To clarify what happened in the first dehydrogenation stage, we analyzed the dehydrogenated residues after the evolution of 0.5 equivalents of H_2 (i.e., $\alpha = 0.2$) by using FTIR spectroscopic analysis (see Figure S9 in the Supporting Information). A sharp peak at around $\tilde{\nu} = 3367.7 \text{ cm}^{-1}$, which may belong to Li-N-H stretch was weakened in the dehydrogenated sample. Simultaneously, the peaks of the C-H stretch that appeared in the low wavenumber range $\tilde{\nu} = 2400\text{--}2713 \text{ cm}^{-1}$ were intensified, thus meaning that some of the C-H bonds in Li_2EDA had been weakened or consumed. On the other hand, two peaks at $\tilde{\nu} = 2097$ and 2029 cm^{-1} , which may belong to the N=C=N stretch in the final product and another C=N stretch in some unknown intermediate, respectively, were observed in the products of Li_2EDA after the release of 0.5 equivalents of H_2 . However, only a strong peak at around $\tilde{\nu} = 2089 \text{ cm}^{-1}$ (assignable to the N=C=N vibration) can be observed after full dehydrogenation at 180°C , thus indicating that some unknown intermediates were formed in the initial dehydrogenation stage. As proposed in our previous work, dehydrogenation of Li_2EDA may be achieved by an α,β -LiH elimination mechanism. It is very likely that the β -H atom first transfers from C to Li, thus forming a N(H)-Li-H moiety and then reacts with the α -H atom on the nearby nitrogen atom to give rise to H_2 and the corresponding [LiCNH] species [Eq. (8)].^[16] That is to say, the migration of hydrogen atoms in the $-\text{CH}_2-$ group and Li^+ ions in $-\text{NHLi}$ group is the rate-determining step of Li_2EDA in the period of $\alpha < 0.25$. In contrast, the calculated Avrami exponent n was higher than 3.5 in the range $0.25 < \alpha < 1$ (Table 3), thus indicating that the three-dimensional growth of nuclei is a rate-limiting process in the main stage of dehydrogenation.



Conclusion

An optimized ball-mill and heat-treatment method for Li_2EDA synthesis was performed in this study. Two intermediates of LiEDA and [LiEDA][Li_2EDA]₂ were observed prior to the formation of Li_2EDA . The phase transformation between partial and dilithiated EDA is reversible. One-dimensional $\{\text{Li}_n\text{N}_n\}$ ladders and three-dimensional network structures were found in LiEDA and Li_2EDA , respectively. Thermal-decomposition studies on these lithiated EDA compounds show that only dilithiated species release high-purity H_2 at elevated temperatures. Thus, the dehydrogenation kinetics of Li_2EDA were systematically investigated by using the Kissinger method, isothermal dehydrogenation experiments, and the JMA equation. The high activation energy ($E_a = 181 \pm 8 \text{ kJ mol}^{-1}$) indicates the significance of temperature in the reaction rate and the high energy barrier to the formation of the transition state. The dynamics mechanism studied by using the JMA method reveals that there are two different rate-determining processes during the dehydrogenation process of Li_2EDA . In the initial dehydrogenation stage ($\alpha < 0.25$), migration of hydrogen atoms in the CH_2 groups and Li^+ ions to optimal positions may be the rate-limiting process. Some unknown intermediates form during this stage, whereas the reaction is controlled by the three-dimensional growth of the final products in the main dehydrogenation stage ($0.25 < \alpha < 1$). These findings provide new trajectories and new methods that can be used for reference in the synthesis, crystallographic studies, and investigation of the thermal behavior of other metalated amines. Moreover, the study of the dehydrogenation dynamics of Li_2EDA may give directive guidance to improve its dehydrogenation properties.

Acknowledgements

The authors would like to acknowledge the Project of National Natural Science Funds for Distinguished Yong Scholar (51225206), 973 Project (2010CB631304), National Natural Science Foundation of China (U1232120 and 51472237), Postdoctoral Science Foundation Funded Project, and the Shanghai Synchrotron Radiation Facility (SSRF) for providing the beam time.

Keywords: amines · crystallization · dehydrogenation · ladder polymers · lithiation

- [1] a) L. Brandsma, H. D. Verkrujse, *Preparative Polar Organometallic Chemistry, Vol. 1*, Springer, Berlin, 1987; b) R. E. Mulvey, S. D. Robertson, *Angew. Chem.* 2013, 125, 11682–11700; *Angew. Chem. Int. Ed.* 2013, 52, 11470–11487; c) F. Mongin, A. Harrison-Marchand, *Chem. Rev.* 2013, 113, 7563–7727; d) A. Harrison-Marchand, F. Mongin, *Chem. Rev.* 2013, 113, 7470–7562.
- [2] M. Lappert, A. Protchenko, P. Power, A. Seeber, *Metal Amide Chemistry*, Wiley, Chichester, 2008.
- [3] a) C. Heathcock, *Stud. Org. Chem.* 1984, 5, 177–237; b) V. Sniekus, *Chem. Rev.* 1990, 90, 879–933; c) M. Beswick, D. Wright, *Comprehensive Organometallic Chemistry II*, Pergamon Press, New York, 1995; d) A.-M. Sapse, P. v. R. Schleyer, *Lithium Chemistry: a Theoretical and Experimental Overview*, Wiley, New York, 1995.

- [4] S. H. Wiedemann, A. Ramírez, D. B. Collum, *J. Am. Chem. Soc.* **2003**, *125*, 15893–15901.
- [5] a) W. Clegg, L. Horsburgh, F. M. Mackenzie, R. E. Mulvey, *J. Chem. Soc. Chem. Commun.* **1995**, 2011–2012; b) R. E. Allan, M. A. Beswick, M. K. Davies, P. R. Raithby, A. Steiner, D. S. Wright, *J. Organomet. Chem.* **1998**, *550*, 71–76; c) D. R. Armstrong, A. Carstairs, K. W. Henderson, *Organometallics* **1999**, *18*, 3589–3596; d) K. B. Aubrecht, B. L. Lucht, D. B. Collum, *Organometallics* **1999**, *18*, 2981–2987; e) K. W. Henderson, P. G. Williard, *Organometallics* **1999**, *18*, 5620–5626.
- [6] D. Seebach, *Angew. Chem.* **1988**, *100*, 1685–1715; *Angew. Chem. Int. Ed. Engl.* **1988**, *27*, 1624–1654.
- [7] a) S. Kanoh, N. Kawaguchi, T. Sumino, Y. Hongoh, H. Suda, *J. Polym. Sci. Part A* **1987**, *25*, 1603–1618; b) Y. Okamoto, T. Nakano, *Chem. Rev.* **1994**, *94*, 349–372.
- [8] P. I. Arvidsson, G. Hilmersson, P. Ahlberg, *J. Am. Chem. Soc.* **1999**, *121*, 1883–1887.
- [9] P. Caubere, *Chem. Rev.* **1993**, *93*, 2317–2334.
- [10] a) P. J. Cox, N. S. Simpkins, *Tetrahedron* **1991**, *2*, 1–26; b) S. G. Davies, O. Ichihara, *Tetrahedron* **1991**, *2*, 183–186; c) J. P. Bégué, D. Bonnetdelpon, M. H. Rock, *Synlett* **1995**, 659–660; d) M. Yus, F. Foubelo, L. R. Falvello, *Tetrahedron* **1995**, *6*, 2081–2092; e) D. M. Hodgson, A. R. Gibbs, *Tetrahedron Lett.* **1997**, *38*, 8907–8910; f) P. O'Brien, *J. Chem. Soc. Perkin Trans. 1* **1998**, 1439–1458; g) T. A. Johnson, D. O. Jang, B. W. Slafer, M. D. Curtis, P. Beak, *J. Am. Chem. Soc.* **2002**, *124*, 11689–11698; h) M. C. Whisler, P. Beak, *J. Org. Chem.* **2003**, *68*, 1207–1215.
- [11] a) R. E. Mulvey, *Chem. Soc. Rev.* **1991**, *20*, 167–209; b) W. Clegg, K. W. Henderson, L. Horsburgh, F. M. Mackenzie, R. E. Mulvey, *Chem. Eur. J.* **1998**, *4*, 53–56; c) N. D. R. Barnett, W. Clegg, L. Horsburgh, D. M. Lindsay, Q.-Y. Liu, F. M. Mackenzie, R. E. Mulvey, P. G. Williard, *Chem. Commun.* **1996**, 2321–2322; d) D. R. Armstrong, D. Barr, W. Clegg, R. E. Mulvey, D. Reed, R. Snaith, K. Wade, *J. Chem. Soc. Chem. Commun.* **1986**, 869–870; e) D. R. Armstrong, D. Barr, R. Snaith, W. Clegg, R. E. Mulvey, K. Wade, D. Reed, *J. Chem. Soc. Dalton Trans.* **1987**, 1071–1081.
- [12] D. B. Collum, *Acc. Chem. Res.* **1993**, *26*, 227–234.
- [13] M. G. Gardiner, C. L. Raston, *Inorg. Chem.* **1996**, *35*, 4047–4059.
- [14] a) P. v. R. Schleyer, A. J. Kos, E. Kaufmann, *J. Am. Chem. Soc.* **1983**, *105*, 7617–7623; b) R. A. Finnegan, H. W. Kutta, *J. Org. Chem.* **1965**, *30*, 4138–4144; c) K. Ziegler, H. G. Gellert, *Justus Liebigs Ann. Chem.* **1950**, *567*, 179–184.
- [15] R. Withnall, I. R. Dunkin, R. Snaith, *J. Chem. Soc. Perkin Trans. 2* **1994**, 1973–1977.
- [16] J. Chen, H. Wu, G. Wu, Z. Xiong, R. Wang, H. Fan, W. Zhou, B. Liu, Y. S. Chua, X. Ju, P. Chen, *Chem. Eur. J.* **2014**, *20*, 6632–6635.
- [17] a) L. Zeng, K. Shimoda, Y. Zhang, H. Miyaoka, T. Ichikawa, Y. Kojima, *Int. J. Hydrogen Energy* **2012**, *37*, 5750–5753; b) P. Chen, Z. Xiong, J. Luo, J. Lin, K. L. Tan, *Nature* **2002**, *420*, 302–304; c) Y. H. Hu, E. Ruckenstein, *J. Phys. Chem. A* **2003**, *107*, 9737–9739.
- [18] G. R. Kowach, C. J. Warren, R. C. Haushalter, F. J. DiSalvo, *Inorg. Chem.* **1998**, *37*, 156–159.
- [19] M. Nagib, H. Jacobs, *Atomkernenergie* **1973**, *21*, 275–278.
- [20] a) D. Blanchard, H. Brinks, B. Hauback, *J. Alloys Compd.* **2006**, *416*, 72–79; b) O. Kircher, M. Fichtner, *J. Alloys Compd.* **2005**, *404*, 339–342.
- [21] J. Christian, *The Theory of Transformation in Metals and Alloys, Part 1: Equilibrium and General Kinetic Theory*, Pergamon Press, Oxford, **1975**, p. 542.
- [22] Certain commercial suppliers are identified in this paper to foster understanding. Such identification does not imply recommendation or endorsement by the NIST.

Received: April 11, 2014

Published online on August 27, 2014